Net Zero Renewable Thermal Energy Solutions for Residential Climate Control:

An Off-Grid Feasibility Study Employing Geothermal Heat Pump and Solar Thermal Energy

Università
Ca'Foscari
Venezia

Samuel Smock
Matricola No. 893450
May 24th, 2022
CM0446 Renewable Energy Sources
Dr. Wilmer Pasut

Abstract:

This paper examines options for renewable thermal climate control systems for a single family off-grid home located in western North Carolina in the United States and evaluates strategies for system sizing, cost control and configuration options based on basic energy balancing. The analysis begins by establishing baselines for solar irradiation, ground temperature, and heating and cooling loads. These numbers are then used as inputs to evaluate two different potential system configurations: a forced air geothermal heat pump running purely on photovoltaic electricity, and a hydronic combisystem with a solar thermal collector and geothermal heat pump ran in parallel with a thermal storage tank also running on PV electric energy.

Each system will be evaluated primarily based off the electric and thermal installed capacity required to cover the energy needs of the system. Capacity and storage sizing are conducted by analyzing two distinct temporal perspectives, a monthly energy budgeting perspective where the hottest and coldest months are examined based on average climatic conditions, and a single day perspective where input and output energy flows are balanced within a cloudy 24-hour period when heating loads are highest and renewable energy input is the lowest. In the monthly analysis, thermal and battery storage are ignored, with the logic that a month is sufficient time for meteorological anomalies to be averaged out. On the daily scale, storage capacity is accounted for and sized based off the amount of energy required to cover a single day deficit. Rather than employing “safety factors” based off a detailed statistical treatment of past meteorological data, various factors along the way are chosen conservatively to achieve a best bet for system sizing

Final recommendations are made regarding the optimal relative sizing of the PV, solar thermal, geothermal and energy storage systems based on the relative cost of commercially available equipment.

TABLE OF CONTENTS

1 INTRODUCTION

Worldwide, heating and cooling accounts for nearly half of all end-use energy consumption and roughly 40% of total carbon emissions (IEA, 2019). In the United States, heating, cooling, and domestic hot water production accounts for over 70% of the end-use energy consumption for single-family, detached homes and is dominated by natural gas as a fuel source (US EIA, 2015). Over the last several decades, air source heat pumps have emerged as a strong option to decrease the energy and carbon intensity of heating and cooling, however their ability to decarbonize residential heating and cooling is limited by the percentage of renewables in the electricity supply and low heating efficiency in cold conditions. Geothermal, ground-coupled heat pumps (GCHPs) and solar thermal heating offer options to decrease carbon intensity, and present strong diurnal and seasonal synergies with one another. However, there are few commercially available products that couple these two renewable thermal energy sources to achieve extremely low energy profiles. This paper will seek to elucidate the state of low carbon, renewable thermal climate control options through a feasibility case study for an off-grid home running a solar PV-powered superficial geothermal heating and cooling system, potentially with solar thermal coupling as well. Many of the findings relating to hybrid solar/geothermal configurations are taken from publications originating from the International Energy Agency's Solar Heating and Cooling Program, (IEA- SHC) Task 44, which investigated solar thermal heat pump systems between 2010 and 2013.

This paper will consider a specific 120 m^2 home design located in western North Carolina in the United States as a baseline for making capacity and sizing calculations, though the technical considerations and general system design recommendations should be easily adaptable to different contexts.

1.1 A NOTE ON UNITS

Because of the unfortunate persistence of the imperial measurement system in the United States and within the heating and cooling industry internationally, an occasional mixture of imperial and SI units will be used here. Heating and cooling loads will often be quoted in British Thermal Units (BTUs), while power inputs from the solar system of thermal solar collection will be quoted in kW. Outside of this, imperial units are avoided, when possible, with an additional exception for insulation metrics which use empirical R values of $ft^2 \cdot °F \cdot h/BTU$. By convention heating load is quoted with a positive sign, while cooling is negative.

2 PROJECT OVERVIEW

2.1 BUILDING DESIGN

The proposed home design is a 133 m^2, entirely off-grid detached structure utilizing PV panels as a primary electricity source. It incorporates several passive heating and cooling features in its' design. Figure 1 highlights these features, namely a reflective metal roof, partially buried first floor and south-facing windows with awnings sized to allow in direct sunlight in the winter, but not in the summer.

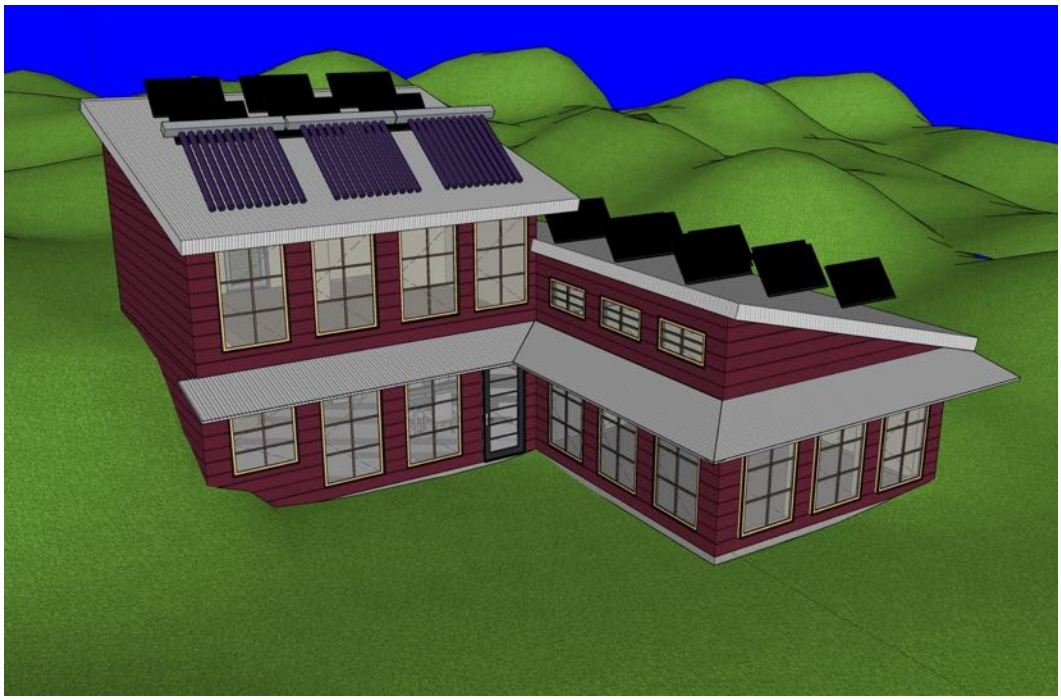

Figure 1: 3-D Model of the house. The entire back wall of the first floor is buried.

2.1.1 Spay foam insulation

The home is designed with closed cell spray foam insulation in the exposed walls and between roof rafters which provides extremely higher insulation value and minimizes vapor transfer into the house by filling small gaps. These features are particularly important for this home design because it lacks an attic and utilizes large numbers of windows to achieve a "greenhouse effect" in the winter.

These products have become popular over the last several decades, but the high global warming potential of hydrofluorocarbon (HFC) blowing agents, which are about 1000 times more potent than CO2, has made it clear that the damage caused by the release of these greenhouse gases during installation and their slow release over time outweighs the efficiency benefits from a

climate change prospective (Johns Manville, 2021a). A new generation of spray foam products which use hydrofluoro-olefin (HFO) blowing agents has recently come on the market. The supposed global warming potential of these is much lower, roughly equivalent to carbon dioxide. For energy calculations on this house, an HFO-blown product released in 2021 called Corobond IV with an R-value of 7 $ft^2 \cdot °F \cdot h/BTU$ per inch is used (John Mansfield, 2021b).

2.2 Climatic Conditions

The proposed project is located in western North Carolina in the United States, a mountainous region with relatively mild, temperate climate. From an interior climate comfort perspective, January represents the most demanding month for heating, with average temperatures of around 1.5 °C and lows well below freezing, while July represents the most demanding month for cooling with an average temperature of 22.4 °C throughout the month and average highs around 27.5 °C (Table 1). Elevated humidity levels around 75% correspond to an average dewpoint of roughly 17.5 °C in the summer which means that dehumidification is an important consideration for the climate control system.[1]

	January	February	March	April	May	June	July	August	September	October	November	December
Avg. Temperature °C (°F)	1.5 °C (34.7) °F	3.4 °C (38.1) °F	7.3 °C (45.1) °F	12.6 °C (54.7) °F	17 °C (62.6) °F	20.9 °C (69.6) °F	22.4 °C (72.3) °F	22.1 °C (71.7) °F	19.2 °C (66.6) °F	13.3 °C (55.9) °F	7.3 °C (45.2) °F	3.4 °C (38.1) °F
Min. Temperature °C (°F)	-2.4 °C (27.7) °F	-0.8 °C (30.6) °F	2.5 °C (36.5) °F	7.3 °C (45.1) °F	11.9 °C (53.5) °F	16.1 °C (61) °F	17.8 °C (64.1) °F	17.6 °C (63.7) °F	14.9 °C (58.8) °F	8.8 °C (47.8) °F	3 °C (37.4) °F	-0.3 °C (31.4) °F
Max. Temperature °C (°F)	7.2 °C (45) °F	9.3 °C (48.8) °F	13.6 °C (56.4) °F	18.9 °C (66) °F	22.5 °C (72.5) °F	26.1 °C (79) °F	27.5 °C (81.5) °F	27.1 °C (80.9) °F	24.3 °C (75.7) °F	18.9 °C (66) °F	13.3 °C (55.9) °F	8.7 °C (47.7) °F
Precipitation / Rainfall mm (in)	103 (4.1)	83 (3.3)	110 (4.3)	94 (3.7)	93 (3.7)	99 (3.9)	106 (4.2)	109 (4.3)	95 (3.7)	89 (3.5)	85 (3.3)	93 (3.7)
Humidity(%)	67%	65%	68%	67%	71%	74%	76%	76%	73%	71%	71%	72%
Rainy days (d)	7	7	8	8	9	11	11	11	8	6	6	7
avg. Sun hours (hours)	6.0	6.3	7.1	8.6	9.3	10.1	9.8	8.9	7.6	6.8	6.5	5.5

Table 1: Monthly Climate Data in Asheville, NC (Climate-Data.org, 2022)

[1] Based on a formula proposed in a 2005 article by Mark G. Lawrence in the Bulletin of the American Meteorological Society, $T_d = T - ((100 - RH) \cdot 0.2)$ - experimentally accurate above 50% RH (Lawrence, 2005).

3 BASELINE PARAMETERS

3.1 SOLAR IRRADIATION

Solar irradiation at the project location is the principal driver of total cost as it determines both the electric output per unit of PV capacity as well as the usable thermal energy produced per unit of installed solar thermal capacity. Working backwards from system energy requirements towards appropriate PV system sizing is a complex process and ultimately comes down to strategic balancing of load, source, and storage and usually involves determining a "safety factor" based off a statistical analysis of past meteorological data together with an acceptable probability threshold for being able to cover demand during long, cloudy stretches of time. For the sake of simplicity, the current analysis will focus instead on energy budgeting on two time frames- monthly and daily. The monthly budget will be established using average monthly conditions to determine the specific yield per unit of capacity in each month. A similar analysis will then be carried out on a daily timeframe, only this time using real irradiation data from 2021 and 2022 to establish a daily energy budget for particularly cloudy days in summer and winter. The daily budget will also be used to determine storage requirements to cover a particularly demanding 24-hour period.

3.1.1 Irradiance, Irradiation, Insolation, Consternation

There is occasionally some confusion that arises as to which type of solar metric to use for what calculation as well as what terms describe *flux* (power per unit area e.g., kW/m^2) versus the time integral of flux, or radiant energy (e.g. kWh/m^2). In this paper, the following conventions are used.

Irradiance – radiant flux or "power", (usually kW/m^2)

Heat flux – sensible energy flux eg. across a wall (BTU/hr/SqFt or kW/m^2)

Irradiation – the time integral of irradiance, used interchangeably with "insolation" (kWh/m^2, often quoted per unit time e.g. Irradiation/day)

Direct Normal Irradiance (DNI) – The amount of solar irradiance received directly from the sun by a surface that is always held perpendicular (or normal) to the sun's rays. This is zero or nearly zero in cloudy conditions.

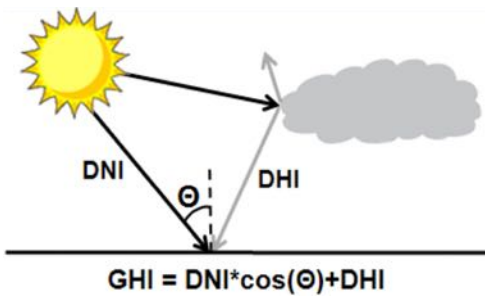

Figure 2: Direct and Diffuse Solar Radiation (Renné, 2018)

Diffuse Horizontal Irradiance (DHI) – Nearly isotropic irradiance coming from atmospheric diffusion. This is the only usable solar energy during full cloud cover.

Global Horizontal Irradiance (GHI) – Used most frequently to calculate solar thermal and PV potential, though an additional factor incorporating panel angle must be applied to the DNI term

3.1.2 A note on panel angle

The solar arrays are designed to face due south and to have a fixed tilt. At a latitude of 36°N, the ideal configuration is a minimum tilt of 12.5° on the summer solstice and 59.5° on the winter solstice (NOAA, 2022). Through experimentation with different tilt angles including options to reset the tilt monthly or quarterly, it was found that simply setting a fixed angle halfway between the two extremes achieved a modest loss of about 5% over the year.[2] The panels are therefore set at a 36° tilt facing due south.

3.2 Monthly Solar Budgeting

On a monthly timescale, the two periods of interest for sizing the climate control system are the coldest and hottest months, July and January. Using data from the US National Renewable Energy Laboratory's (NREL) PVWatts calculator and default values for system losses of 14%, a rough picture of expected DC energy yield per kilowatt of installed capacity was obtained. This data was additionally used to calculate the thermal energy per square meter of an evacuated tube solar thermal collector. The data is summarized in Table 2.

3.2.1 PVWatts Solar Energy Calculator

The PVWatts solar capacity calculator creates daily averages by running an hourly performance simulation using a typical-year weather file from one of three national solar radiation databases representing multi-decade historical periods.[3] The process sums the normal component of DNI with DHI on an hourly basis to determine irradiation totals across a fixed angled surface as shown in Equation 1 (Dobos, 2014).

Eq. 1

$$Radiant\ Flux\ Fixed\ Panel = DNI \cdot \cos(AOI) + DHI$$

$$= DNI \cdot [\sin(\theta_{sun}) \cdot \cos(\gamma - \gamma_{sun}) \sin(\beta) + \cos(\theta_{sun}) \cdot \cos(\beta)] + DHI$$

Where β is panel tilt, γ is panel azimuth (180° if due south), γ_{sun} solar azimuth, and θ_{sun} solar zenith. Together these comprise the angle of incidence (AOI) which changes throughout the day and year.

[2] This result comes from comparing a constant 36-degree tilt with one that resets monthly to the optimal angle in the NREL PVWatt calculator.

[3] The three solar resource databases are National Solar Radiation Database (NSRDB) 1961-1990 data (TMY2) and 1991-2010 update (TMY3), and EnergyPlus weather files. Unfortunately, PVWatts does not reveal to the user which data set are used when, but surely several decades of weather data are incorporated

The calculator also allows the user to insert information on the type of solar panel to estimate thermal solar panel loss using actual temperature data. In Table 2, specific monthly DC yield is calculated directly from radiation data rather than listing PVWatts' AC energy figures to allow for the system the option of using DC equipment and pumps.

Month	Average Daily Solar Irradiation Perpendicular to Panel @ 36 Degrees[4] ($kWh/m^2/day$)	Specific Monthly PV Yield[5] (kWh/kW_p)	Solar Thermal System Efficiency[6]	Specific Monthly Thermal Yield (kWh/m^2)
January	4.36	114.25	0.45	59.78
February	4.91	128.78	0.4	59.90
March	5.29	138.86	0.5	80.73
April	5.60	146.84	0.55	93.91
May	5.79	151.76	0.6	105.88
June	5.99	157.05	0.55	100.44
July	5.63	147.74	0.5	85.90
August	5.90	154.69	0.5	89.94
September	5.67	148.68	0.5	86.44
October	5.37	140.93	0.5	81.93
November	4.70	123.21	0.45	64.47
December	3.83	100.39	0.4	46.69

Table 2: Monthly Average of Solar PV and Thermal Energy Output in Asheville, NC with a 36^p fixed tilt panels

3.2.2 Solar Thermal Collector

For this project, the type of thermal solar collector considered is a heat pipe evacuated tube collector (HP-ETC) paired with a forced recirculation loop connected to a buffer tank. The solar thermal efficiency of these systems depends on a variety of factors mostly related to climatic conditions. For instance, Widyolar et al. (2021) established a strong relationship between thermal efficiency and the difference between mean operating liquid and ambient temperatures, implying an unfortunate drop in efficiency in winter when heat is needed the most. Furthermore, specific system parameters such as supply pipe thermal loss introduce somewhat wide ranges of expected system thermal efficiency. For the purposes of establishing a baseline, this paper will use the

[4] Solar Irradiation per day is calculated by PVWatts by combining angle of incidence (AOI) with DNI and DHI to obtain energy flux through a tilted surface and summing over the course of the day (US NREL, 2022).

[5] Usable DC output from PV arrays with 14% loss from soiling, self-shading, voltage mismatch between panels, wiring, connections, nameplate inaccuracy, and system downtime. 1 kW_p installed capacity yields 1 kWh/h under "Standard Test Conditions" of 1 kW/m2, therefore the average daily numbers can just be multiplied by 30.5 to get average monthly values.

[6] (Ayompe & Duffy, 2013)

results from a study undertaken in Dublin in 2010 showing a range of system solar-thermal efficiency of around 40% in winter and around 60% in summer, including all thermal losses at the collector and in the supply lines when operating at in the range of domestic use hot water temperatures, around 50ºC (Ayompe & Duffy, 2013). Though we are only concerned with the performance in mid-winter for climate control, table 2 has been populated with values from the Dublin study to provide representative values year-round.

3.3 Daily Solar Budgeting

Detailed hourly solar radiation data from the last year from the Solcast data set was used to pinpoint specific days in the months of January and July that represented the most demanding conditions from an energy budgeting standpoint. Figures 3 and 4 summarize the irradiation data from those months and identify January 16th, 2022, and July 20th, 2021, as days for this "worst case" analysis.

As can be seen in the figures, no DNI was measured at all for either of these dates meaning PV panels and solar thermal collectors only pick up diffuse radiation during these days. This eliminates the need for hourly angle of incidence calculations. Power and thermal output can therefore be calculated as a simple product of summed hourly DHI, PV array capacity, and solar thermal system efficiency.

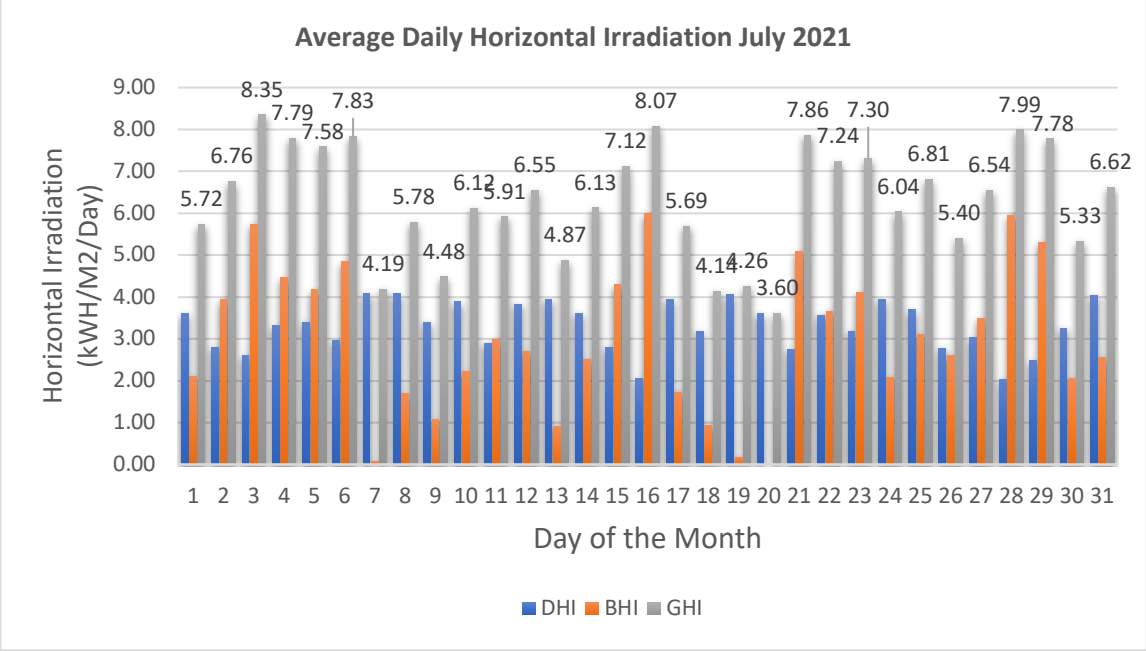

Figure 3- July Daily Irradiation Totals derived from hourly GHI (Solcast, 2022)

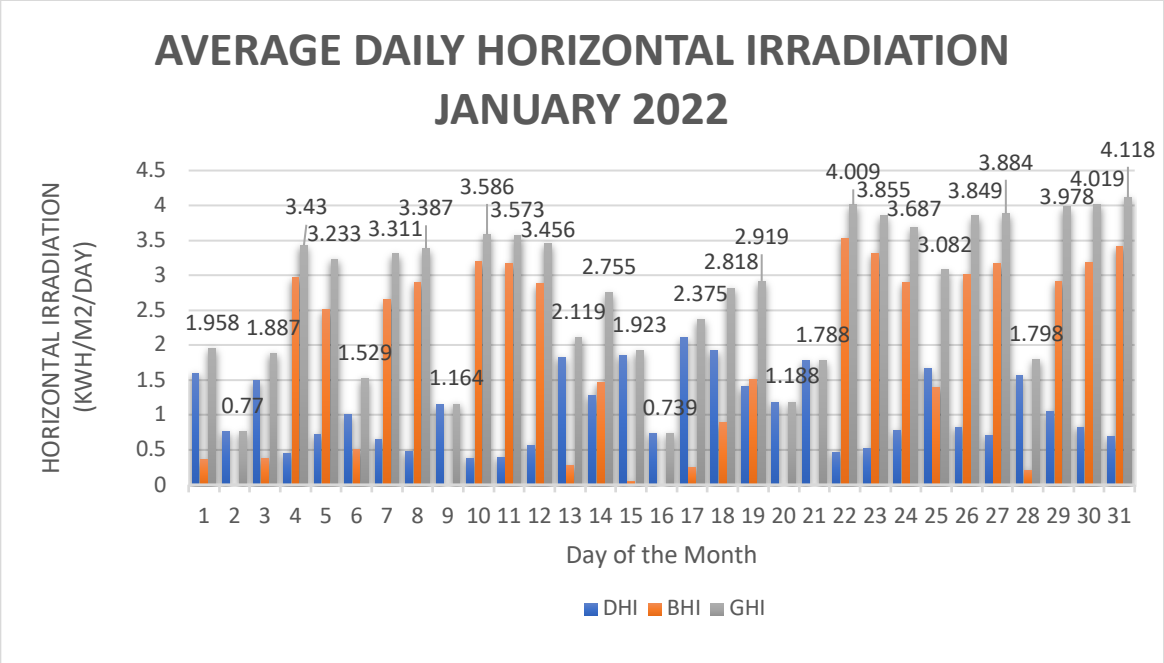

Figure 4 – January Daily Irradiation Totals derived from hourly GHI (Solcast, 2022)

Using the same efficiency numbers from the monthly budgeting section yields numbers for daily PV and thermal energy output on these two dates. These numbers are summarized in table 3.

Date	**Daily Solar Irradiation Perpendicular to Panel @ 36 Degrees[7] (kWh/m²/day)**	**PV Yield (kWh/kW$_p$/day)**	**Solar Thermal System Efficiency[8]**	**Specific Monthly Thermal Yield (kWh/m²*day)**
January 16th, 2022	0.74	0.64	0.45	0.33
July 20th, 2021	3.6	3.10	0.5	1.8

Table 3- Daily Solar PV and Thermal Energy Output in Asheville, NC with 36º fixed tilt panels

3.4 Ground Temperature Profile

Estimating ground temperature gradient with depth in a precise way is difficult without taking empirical measurements on site, so a literature review focused on identifying field studies in similar climates and soil types was undertaken to arrive at a sinusoidal approximation for

[7] Hourly summed DHI (equivalent to GHI on these days)
[8] (Ayompe & Duffy, 2013)

temperature at a depth of 3m over the year and to create a best guess for ground temperature as a function of depth in midwinter and midsummer.[9] These equations can then be matched with well water temperature surveys, to achieve workable figures. Using 1989 study in Alabama, United States, a national well water temperature survey, and a 2013 study in Maslak, Turkey, the following equations were derived.[10][11]

Eq. 2 $$T(t) = 15℃ - \ 2.5℃ * \ \sin\left(\frac{t-14}{365}2\pi\right)$$

Matching this with climate data yields a linear approximation of temperature at a depth of d meters in January:

Eq. 3 $$T(d) = 1.5℃ + 4.5\left(^{℃}/_{m}\right) * d \quad ; \quad 0 < d < 3 \ ; \ January$$

and in July:

Eq. 4 $$T(d) = 22.4℃ - 2.5\left(^{℃}/_{m}\right) * d. \quad ; \quad 0 < d < 3 \ ; \ July$$

Equations 3 and 4 will be useful in determining heat flux across the walls in the buried portion of the house, while Equation 2 will later be used to evaluate the performance of the heat pump.

3.5 Heating and Cooling Loads

Having established geothermal and solar metrics to be used as inputs to the renewable thermal climate control system, the analysis now requires heating and cooling loads to approximate sensible energy "consumption." There is a well-documented tendency for the industry to oversize climate control systems which results in larger installation costs, operational costs, and

[9] Temperature profiles in mid-winter and mid-summer are monotonic and relatively flat making a linear approximation reasonable for this time of year only. Spring and fall season changes on the other hand lead to inversions and more complicated profiles. See Appendix A.

[10] Equations were deduced first by noting that both studies showed a seasonal variation of around +/- 2.5oC around the mean at 3m, then establishing an annual mean earth temperature of around 15oC from well water temperature surveys. From there, average surface temperatures in January and July were fit with the prediction of temperature at 3m from the sinusoidal model to obtain a linear temperature gradient. Detailed figures from these studies and additional discussion can be found in the appendix.

[11] The phase term of roughly two weeks is in place to fit the approximation to the observed minimum temperature at 3m in the second week of April. See Appendix.

higher electricity consumption (NREL, 2011). Accurate thermal load sizing is an entire discipline unto itself, and the details are beyond the scope of this paper. For this reason, two baselines were used to establish reasonable upper and lower bounds for the building under consideration. For the upper bound, a commercial online calculator was used which incorporated building size, the number of windows and the climate zone, but no other passive heating and cooling features of the building itself. For a lower limit tailored to the study climate, a building energy balance analysis was conducted incorporating the insolation of proposed materials, climatic conditions, ground temperature approximations, as well as solar irradiation data to approximate radiative effects. This analysis was conducted for the January 16th and July 20th following the results above.

3.5.1 Commercial Peak Load Calculator

A wide variety of online calculators are available for heating and cooling load calculations. They incorporate only general properties of the building such as floor area and number of windows and tend to produce similar results. The calculator from highseer.com was chosen and produced the following numbers with the given inputs:

PARAMETER	VALUE
CLIMATE ZONE	#3 – Mixed-humid
AREA (SQFT)	1440
INSULATION GRADE	Extremely well insulated
SUN EXPOSURE	Shaded or Interior
NUMBER OF WINDOWS	More than Average
WINDOW AND DOOR AIR TIGHTNESS	Double Pane Well Sealed
OCCUPANTS	2 or less
KITCHEN	Yes
SPACE HEIGHT	9 ft.
HEATING LOAD	36,000 BTU
COOLING LOAD	37,700 BTU

Table 4: Commercial Heating/Cooling Load Calculator Inputs and Outputs (HighSeer, 2022)

3.5.2 Energy Balance Method for Capacity Calculating

An energy flux calculation was also carried out to provide a point of comparison to the online calculator as well as a daily snapshot of thermal loads. Passive heating and cooling features of the building, such as the reflective roof, dug-in construction, and awnings are incorporated through material R values, radiative heat pickup and the insulating effect of partial burial. This analysis is summarized in table 5.

MATERIAL	R- VALUE[12] $\frac{(ft2 \cdot ^\circ F \cdot h)}{BTU}$	AREA (FT^2)	INDOOR TEMP (F)	AVG.[13] JULY HIGH (F)	AVG.[13] JAN. LOW (F)	JAN. 16TH HEAT TRANSFER (BTU/HR)	JULY 20TH HEAT TRANSFER (BTU/HR)
CONDUCTIVE HEAT LOSS/GAIN							
INSULATED EXTERIOR WALL (5.5" @ 7R/INCH)	39	1515	68	82	28	-1586	531
DOUBLE PANE WINDOWS WITH 3/4" AIR SPACE	2	324	68	82	28	-5486	1838
SOLID INSULATED METAL DOOR	10	43	68	82	28	-173	58
REFLECTIVE METAL ROOF, CLOSED FOAM INSULATED RAFTERS (R7/INCH @ 7.5")	53	1200	68	82	28	-921	309
6" CONCRETE WALL (BURIED)	1	522	68	70	43	-10461	976
CONCRETE FLOOR 6"	1	1044	68	70	43	-20922	1952
RADIATIVE HEAT GAIN[14]							
DOUBLE PANE WINDOWS @ 0.739KWH/M2/DAY DHI[15]		324				2910	
DOUBLE PANE WINDOWS @ 3.6KWH/M2/DAY DHI		324					14176
HEATING/COOLING LOAD (BTU/HR)						-36640	19309

Table 5: A summary of the values used to Approximate Heating and Cooling Loads using Energy Flux

[12] Representative numbers from industry toolboxes (Johns Manville, 2021a) (ArchToolBox, 2022)

[13] The below ground portion integrates the linear ground temperature approximation from the previous section. Total heat transfer, $\dot{Q} = -\int k \cdot \Delta T(x,y) dA$, which is mathematically equivalent to $\dot{Q} = -k \frac{\int \Delta T(x,y) dA}{A} A = -\frac{1}{R} \cdot \bar{T} \cdot A$. Therefore, average ground temperatures across each subterranean surface extent are presented in the table here

[14] Only DHI through windows is listed here because on these days DNI is zero and radiative absorption through the roof is considered negligible because of reflective roofing and minimal transfer absorbed radiative heat at the roof due to high r value sub roofing material. On other days more terms for exposed walls and roofing would appear.

[15] Cumulative DHI from July 21st, 2021, and January 16th, 2022, respectively (Solcast, 2022)

While the heating load of around 37,000 BTU calculated in this manner is strikingly close to the value given by the online calculator, the cooling load is significantly lower, owing to the high insulation factors in the above ground portion of the house and insulating effect of partial burial.

3.5.3 Peak load Synthesis and Energy Consumption

The two methods above established a window for the home's *peak* heating and cooling load around 35-36 thousand BTU/HR heating and around 19-38 thousand BTU/HR cooling. However, to make a direct energy balance with electric energy input, these figures must be converted to energy consumption on a monthly and daily timeframe, a process that is highly dependent on system boundary conditions such as climate, source/sink temperature, and user behavior. Constraining the consumption of a given system indeed represents one of the major hurdles in comparing different systems and field studies as was noted by Haller et. al. in their reports on solar heating and cooling for the IEA SHC Task 44 (2014).

To achieve usable average daily and monthly energy *consumption* figures, peak load and insulation factors were compared with studies of similarly constructed buildings in similar climates following the reference framework for system simulations of the IEA SHC Task 44 which used baseline homes in 3 different cities (Dott, et. al. 2013). Strasbourg, France was chosen as a comparison climate because January average temperature there is the closest to the climate in the study area (2.3 ^{o}C compared to 1.5^{o}C in that in Asheville, NC) (Climate-Data.org, 2022).

The insulation values and peak loads from above calculations were found to be most similar to a well-insulated, light construction home (SFH15) in the reference classification scheme. This corresponds to a January net thermal energy requirement of 5.5 kWh/m^2 or 731.5 kWh for the 133 m^2 home (Dott, et. al. 2013).

It should be noted that this figure could be an overestimate because the winter solar irradiation incident on a south facing wall in Strasbourg is roughly half of what it is in Asheville, NC due to its' higher latitude and cloudier winter climate (Solcast, 2022)(Dott, et. al. 2013). Nevertheless, the conductive portion of the heat transfer is taken to be a close match, and certainly fits for the cloudy daily analysis, so figures from the Strasbourg study are taken as a representative value for heating requirements.

There are much fewer field studies relating to cooling system load factors, though it will be seen in the next section that for the purposes of PV system sizing, winter heating is the constraining factor, not summer cooling. For this reason, a similar load factor (energy consumption/capacity @ fulltime operation) of about 10% is used for cooling values in the summer to yield a rough estimate of the *excess energy* the system will produce in the summertime.

4 SYSTEM CONFIGURATIONS

Both the geothermal heat pump and solar thermal/geothermal combisystem can now be presented and analyzed using the baseline information determined above. Table 6 summarizes the baselines derived in section 3, with sensible heat figures translated to metric equivalents.

		WINTER		**SUMMER**	
		January (LTA)	Jan 16th, 2022	July (LTA)	July 20th, 2021
INPUTS (SPECIFIC YIELD)	PV	109.68 $(\frac{kW}{kW_p})$,	0.61 $(\frac{kW}{kW_p})$,	141.83 $(\frac{kW}{kW_p})$,	2.98 $(\frac{kW}{kW_p})$,
	Sol. Therm.	59.78$\left(\frac{kW}{m^2}\right)$	0.34 $\left(\frac{kW}{m^2}\right)$	85.90 $\left(\frac{kW}{m^2}\right)$	1.80 $\left(\frac{kW}{m^2}\right)$
OUTPUTS HEATING/ COOLING	Sensible	731 (kWh)	24 (kWh)	-766 (kWh)[16]	- 13 (kWh)[17]

Table 6; Summary of heating and cooling loads and solar energy uptake

4.1 GROUND SOURCE HEAT PUMP AND PV

This configuration is the simplest of those considered here and has the benefit of many turnkey products from a rather mature market. In this configuration, electrical energy from PV panels and battery storage are ran through an inverter and used to power an off-the-shelf residential geothermal heat pump and air handler (Figure 5). In line with peak load calculations from the prior section, the Bosch SM036-1CS water-to-air heat pump paired with a SM036-1AH air handler was used as a representational model for energy calculations. Determining accurate seasonal performance factors (SPFs) can be difficult even with well-established products because input temperatures quoted for closed loop configurations in system specifications sheets tend to be quite a more pessimistic than those predicted in equation 2 above. Indeed, one chief advantage of this system is that seasonal peaks and troughs of the ground temperature are offset from the surface temperature by about 3 months. A fact which is exploited for heating and

[16] LTA January sensible heat consumption comes from the Strasbourg study. Other loads are approximated by using a similar load factor with peak loads calculated in each timeframe. Summer numbers should thus be treated as rough estimates. Negative sign indicates removing heat.

[17] Note that the daily cooling load for July 20th is much lower than the monthly average because of low radiant uptake for that day

cooling. For this reason, a winter COP of 5.7 and a summer EER of 37 for a partial load and inlet temperature of 59 ºF (15 ºC) are extrapolated from product technical specifications by way of interpolation (Bosch, 2015). While these are best guess values, they are consistent with ground water temperature/COP pairs listed in the manufacture tables, as well as experimental findings of a 2-3% drop in COP for each degree of temperature sink decrease (Haller, 2014).

Each potential system configuration will be presented schematically using a modified form of the energy flow diagram used by the IEA-SHC Task 44 with renewable power inputs in the left column, ambient heat sources on the top, and end-use sensible heat on the right. The energy flow for the Ground Coupled Heat Pump (GCHP) system is diagramed below.

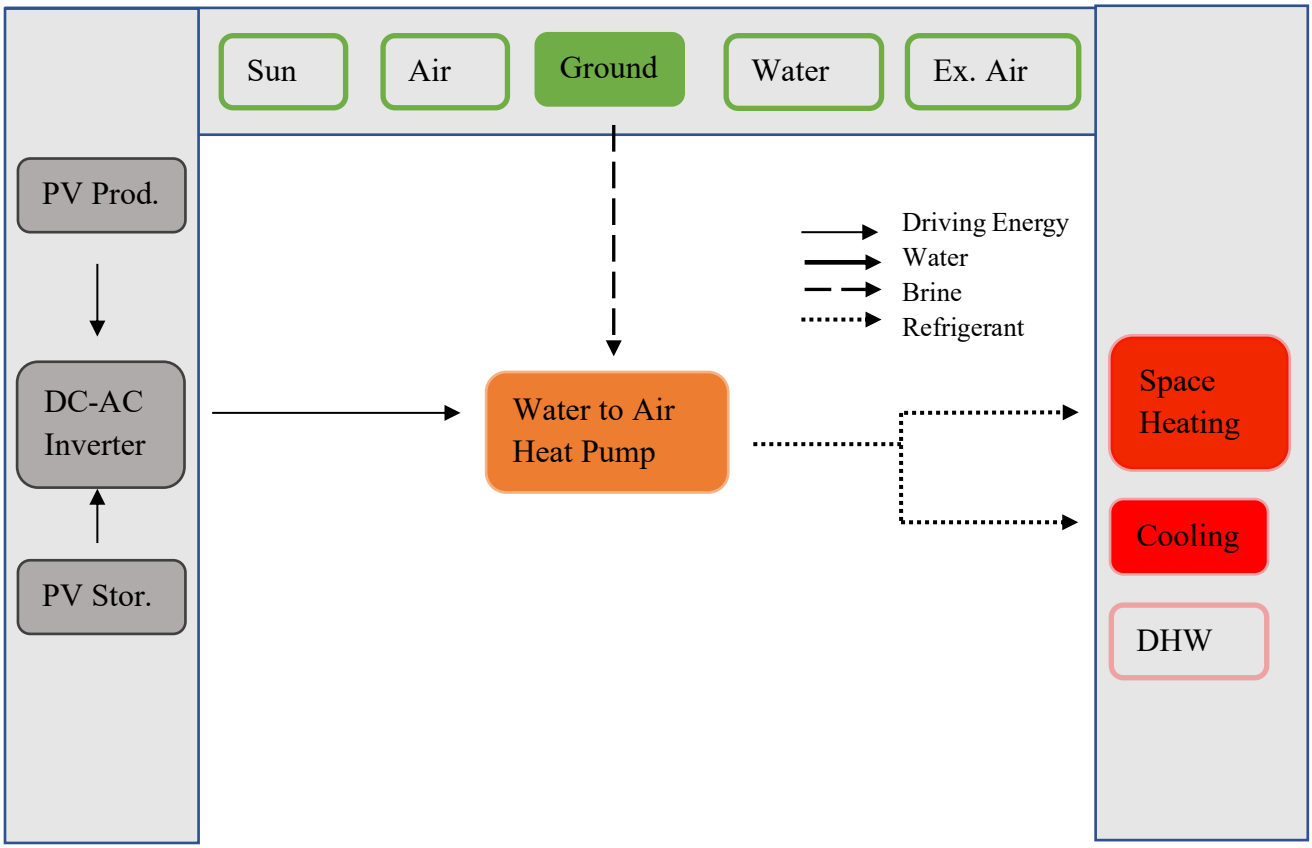

Figure 5: Energy Schematic of Off-Grid Ground Source Heat Pump with Forced Air Heating/Cooling in the style of IEA-SHC Task 44 Energy Flow Chart

The other major energy cost of this set up is the large blower in the air handler. Rather than treat this as a separate term in the energy balance equations, a technical reference sheet providing the combined heat pump/air handler SPFs was used to infer a general approximation of the decrease in system performance from the blower. Comparing this literature, these were found to be about 0.25 COP and 10 EER, Leaving a final $COP_{GCHP,HVAC}$= 5.45 and $EER_{GCHP,HVAC}$ = 27 (Bosch,

2021) This result shows that blower energy usage, which is roughly constant seasonally, is proportionally much lower in the winter as heating is more energy intensive than cooling.

4.1.1 Energy Balance

The overall energy balance of the system is described by equations 5 and 6

eq. 5

$$Q_{HEAT} = Q_{GCHP}$$

$$\int \dot{Q}_{heat} dt = COP_{GCHP,HVAC} \cdot (E_{PV} + E_{Stor.}) \cdot \eta_{ACDC}$$

And

eq. 6

$$Q_{COOL} = Q_{GCHP}$$

$$\int \dot{Q}_{cool} dt = EER_{GCHP,HVAC} \cdot (E_{PV} + E_{Stor.}) \cdot \eta_{ACDC}$$

Where Q_{heat} and Q_{cool} are the cooling and heating loads from table 6 above, $COP_{GCHP,HVAC}$, and $EER_{GCHP,HVAC}$ are combined heatpump/air handler SPFs from product literature, and η_{ACDC} is the efficiency of the home's inverter, taken to be 95% following the PVWatts calculator and commercially available examples. E_{pv} was determined empirically in section 3 above and is mathematically given by integrating equation 1.

Using values from table 6, and the above equations, solar system sizing can be done. The results of this analysis are summarized in table 7.

	Winter		Summer	
	January (LTA)	Jan 16th, 2022	July (LTA)	July 20th, 2021
Outputs				
Net Heating/Cooling Thermal Energy (kWh)	731	24	769	9
DHW (kWh)[18]	173	6	173	6
Lighting, Refrigeration and Appliances (kWh)[19]	269	9	269	9
Conversion Factors				
SPF (COP and EER)[20]	5.45	5.45	27.00	27.00
Heating/Cooling Electrical Energy (kWh - AC)	134.13	4.40	28.48	0.33
Heating/Cooling Electrical Energy (kWh - DC)	141.19	4.64	29.98	0.35
Specific PV Yield (kWh/kWp)	114.25	0.64	147.74	3.10
Inputs and Storage[21]				
PV Capacity Required - house (heat pmp) (kWp)	4.75 (1.24)	-	2.99 (0.20)	-
Battery Storage Required (Daily Deficit) (kWh)	-	19.21 (3.84)	-	15.09 (0.10)
Battery Storage (aH at 48V)	-	400 (80)	-	314.48 (2.09)

Table 7: Energy Balance for a PV powered Ground Source Heat Pump

PV capacity was determined by using the long-term monthly averages of solar radiation and heating energy consumption from table 6 to determine the PV capacity needed to cover the average month. Cloudy day scenarios were then used to calculate a minimum storage size needed to cover the deficit of a 4.75 kW_p PV system.

[18] Assuming equal monthly usage of an electric hot water heater over a year (Haller, 2014)

[19] Using average American single-family home and end use energy breakdown (US EIA, 2015) (US EIA, 2021)

20 Includes the air handler.

21 The figures in the "Inputs and Storage" section of table 7 show the whole home's energy needs and the portion of which is used by the heat pump in parentheses.

The main conclusions from this analysis are that winter is by far the most energy intensive season for climate control. Furthermore, this system is particularly sensitive to cloudy winter days where heating needs are highest and PV production is lowest as evidenced by the roughly 4 kW battery requirement just for the heat pump. In this model, heating accounts for about 26% of the electrical use of the house for the month of January.

4.2 Ground Source and Solar Thermal Parallel Combisystem

This configuration incorporates a solar thermal collector and storage tank with a backup liquid to liquid heat exchanger for winter radiant floor and/or fan coil heating and domestic hot water (DHW). In the summer, the ground source heat pump runs chilled water to fan coil coolers. The system is now entirely hydronic, and the energy sources operate in parallel. Because the system is now responsible for domestic hot water, the system is set to 50 ºC to protect against legionella, which is reflected in the heat pump COP and thermal collector efficiency. The energy flow diagram for this system can be seen in figure 6.

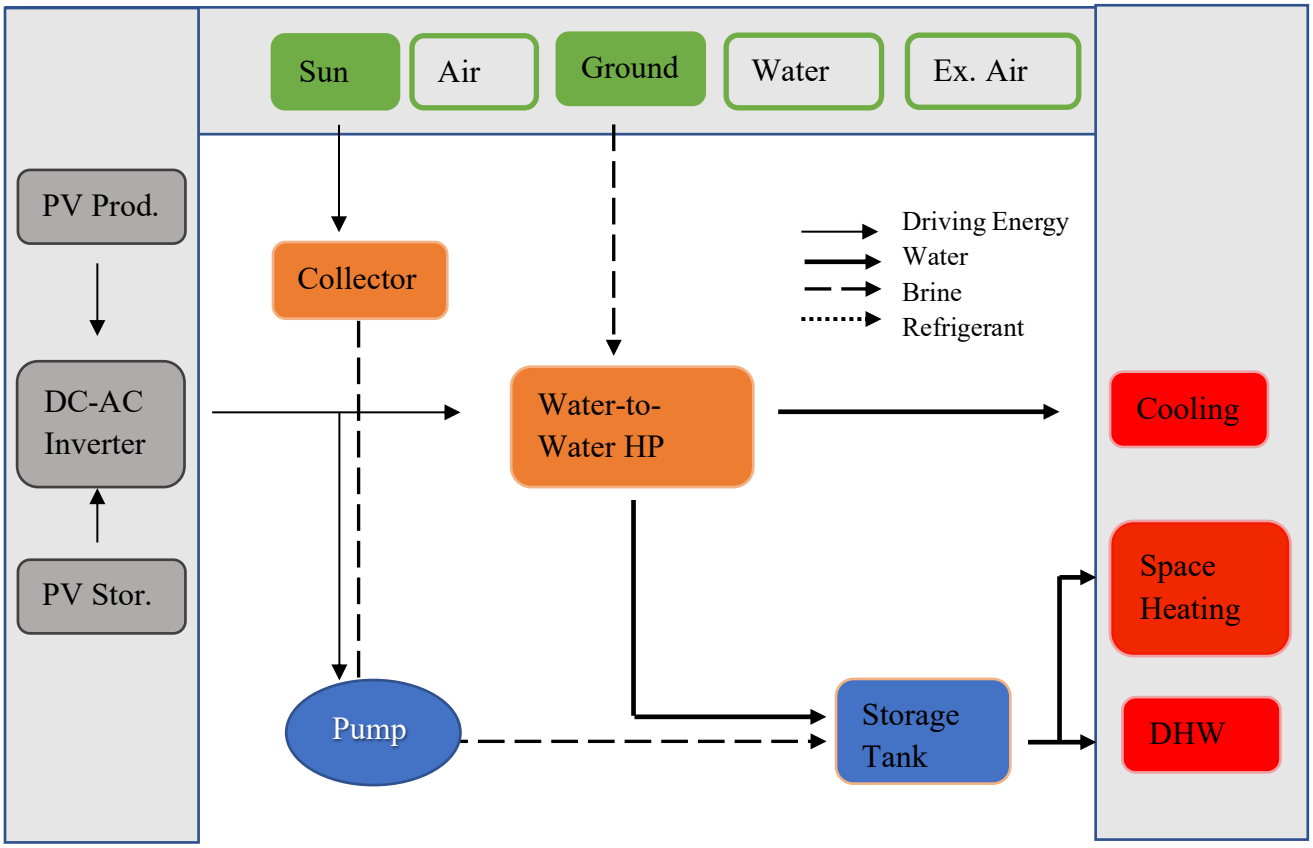

Figure 6: Energy Flow Diagram of The Solar Thermal/GCHP Combi System Ran in Parallel

4.2.1 Energy Balance

The balance equations for this system are similar to those for the last configuration, but with an added term for solar collectors on the right.

eq. 7

$$Q_{HEAT} + Q_{DHW} = Q_{GCHP} + Q_{SOL} - E_{pump}$$

$$\int \dot{Q}_{heat}\, dt + Q_{DHW} = COP_{GCHP,50,} \cdot (E_{PV} + E_{Stor.}) \cdot \eta_{ACDC} + (Q_{COLL} + Q_{THERM}) - E_{pump}$$

And

eq. 8

$$Q_{COOL} = Q_{GCHP,50} - E_{pump}$$

$$\int \dot{Q}_{cool} dt = EER_{GCHP} \cdot (E_{PV} + E_{Stor.}) \cdot \eta_{ACDC} - E_{pump}$$

The reference unit used for these calculations was the Bosch WT035 water to water heat pump. Using the technical specifications and again extrapolating based off a 2% per ºC improvement in COP to match January and July Ground Temperatures, the operational SPFs were found to be $COP_{GCHP,50}$ of 4.1 and an EER_{GCHP} of 21.78. These figures do not include additional pumps or effects from variation in specific heat capacity from propylene glycol in the brine but do reflect a higher set point of at least 50 ºC for domestic hot water.

Sizing is considerably more complicated than in the last configuration because there are now two variable energy inputs- thermal and PV, and two fixed storage reservoirs- a hot water tank and a battery bank. The method used to confront this is based on the greatly reduced electric profile of thermal collectors, which collect about ten times more heat per electric input as heat pumps (Haller, 2014). Therefore, sizing was done in such a way that the long-term average heating and hot water needs in January were fully covered by the solar collector, and the tank was sized to bridge the deficit of January 16th when there was very little sunlight. The PV and battery system were sized similarly to cover the homes' non-heating electrical needs with the understanding that the electric system can also be used to run the geothermal heat pump as an additional backup.

The results of the energy balance analysis for the Solar Thermal and Geothermal Combisystem are summarized in table 8.

	Winter		Summer	
	January (LTA)	Jan 16th,2022	July (LTA)	July 20th, 2021
Outputs				
Net Heating/Cooling Sensible Heat (kWh)	731	24	769	9
DHW (kWh)	173	6	173	6
2 x 4lpm DC Water pumps[22] (kWh)	42	2	42	2
Lighting, Refrigeration and Appliances (kWh)	269	9	269	9
Conversion Factors				
SPF (COP and EER)	4.10	4.10	21.78	21.78
Specific Solar Thermal Energy (kWh sensible heat/ m2)	59.78	0.33	85.90	1.80
Specific PV Yield (kWh/kWp)	114.25	0.64	147.74	3.10
Inverter Efficiency	0.95	0.95	0.95	0.95
Inputs				
Solar Thermal Capacity Required (m2 ETC)	15.12	-	2.01	-
Thermal Storage Capacity (kWh)	-	25.01	-	11.37
Thermal Storage Capacity[23] (liters H2O @ 50C)	-	717.02	-	326.11
PV Capacity Required (kWp)	2.84	-	2.45	-
Battery Storage Required (Daily Deficit) (kWh)	-	9.13	-	3.08
Battery Storage (aH at 48V)	-	190.26	-	64.18

Table 8:Energy Balance Analysis for a GCHP/Solar Thermal Parallel Combisystem

As with the GCHP system, winter is the energy bottleneck with this system, though the amount of electric power required in the winter vs summer is now much closer. The addition of the solar thermal collector and thermal storage allows the PV System to be designed with 40% lower

[22] Two 70W, 4 lpm pumps running a total of 20 hrs. / day (8 for solar thermal collector, 12 for radiant heating loop)

[23] Heat Capacity of water = 4.19 J/g*°C = 0.00116 kWh/l*°C ; $\Delta T = 30$ ℃

capacity and 52% lower battery storage. Because the heat pump still must provide all the cooling in the summer, the inverter size will be likely similar.

4.2.2 Cost comparison

While the overall efficiency of the system is certainly improved with the addition of solar thermal heating, the saved costs on the PV side may be outweighed by the addition of extra equipment like the tank, collector and radiant heating. To get a general sense of the cost performance, the saved cost on the PV side can be compared with the added costs on the thermal side using rough cost estimates to products available directly to the consumer in the US. This cost breakdown is summarized in Table 9.

	GCHP	GCHP/SOLAR THERMAL COMBI SYSTEM	UNIT COST ($)[24]	DIFFERENCE ($)
PV PANELS (KW_P)	4.75	2.84	1250	-2387
LI-ION BATTERY STORAGE (KWH)	19.21	9.13	500	-5040
ETC SOLAR THERMAL (M^2)	0	15.12	550	8316
BUFFER TANK (L)	0	750	2	1500
TOTAL				2389

Table 9: Cost breakdown of swapping PV Capacity for Solar Thermal Capacity

The cost breakdown shown here relies on a variety of major assumptions such as a rough cost parity for a water-to-water vs water-to-air heat pump and similar cost breakdowns for ductwork and piping for radiant hydronic heating. It also omits various other minor costs and differences in maintenance. However, the analysis does suggest that for such a small building, the inclusion of solar thermal heating may not be worth the added up-front costs. It is likely that this may have an inflection point as the building size gets larger for instance in a multi-unit residential or light commercial situation.

[24] These numbers are rough estimates from a survey of products available directly to consumers in the US from renogy.com, gogreensolar.com, buildclub.com, and dudadiesel.com among others.

5 Conclusion and Further Considerations

This paper conducted a detailed analysis on two potential setups for the climate control of a single family, off-grid home in western North Carolina in the United States. The basic principle underlying the system is a renewable source of electric energy which powers a renewable thermal heating and cooling system. While the two configurations explored here highlighted PV as an electric energy source and geothermal/solar thermal as an ambient source of thermal energy, myriad other combinations exist. Of particular interest for further investigation are other sources of electric energy such as wind or micro hydro that do not suffer from the strong negative correlation with winter heating loads that solar does. Additionally, variations on the internal routing of thermal carriers could provide interesting opportunities to pick up additional efficiencies. One such variation would involve geothermal and solar thermal systems routed in series whereby geothermal input brine is preheated by solar thermal storage and chilled outlet brine is used as an input for the solar thermal collector, which would increase the operating efficiencies of both systems in heating mode. A completely passive system that has no heat pump and just uses solar thermal for heating and a geothermal loop through a fan coil for cooling could also cover a significant portion of the homes' climate control needs, particularly if set temperatures are less stringent and/or backups for the most extreme heat and cold are employed.

In this analysis, the treatment of the statistical spread of solar energy available to the home was simplified by sizing the system based off monthly and daily timeframes for energy coverage. Rather than establishing a statistical threshold for the probability of covering the home's energy needs during anomalous meteorological periods, the system was sized by analyzing the average conditions in peak heating and cooling months, and subsequently tested for particularly cloudy days in those months. Additional statistical treatment of the system sizes presented here could well be conducted to add a "safety factor," though the sizing presented here can be regarded as already quite conservative due to various parameter choices along the way.

The conclusion regarding which of the two systems is best suited for this project is that the simpler system employing only geothermal energy and a heat pump would be the cheapest to install and would result in a hefty surplus of electricity during the summertime. On the other hand, the inclusion of solar thermal energy input would increase installation costs but result in a leaner and more energetically efficient system as a whole. The effects of system size are likely key to this conclusion, and a similar treatment of larger or grid-tied buildings running similar renewable thermal climate control systems would likely show a wide benefit to pairing numerous ambient thermal heat inputs.

6 REFERENCES

Airaksinen, M., & Vuolle, M. (2013). *Heating Energy and Peak-Power Demand in a Standard and Low Energy Building*. Retrieved from Energies, 6, 235-250: doi:10.3390/en6010235

Alternative Energy Tutorials. (2022). Retrieved from https://www.alternative-energy-tutorials.com/photovoltaics/standard-test-conditions.html#:~:text=The%20standard%20test%20condition%20for,of%201.5%20(1%20sun).

ArchToolBox. (2022). Retrieved from https://www.archtoolbox.com/r-values/

Aydin, M., Sisman, A., Gültekin, A., & Dehghan B., B. (2015). *An Experimental Performance Comparison between Different Shallow Ground Heat Exchangers*. Retrieved from World Geothermal Conference: https://www.researchgate.net/publication/286456011_An_Experimental_Performance_Comparison_between_Different_Shallow_Ground_Heat_Exchangers

Ayompe, L., & Duffy, A. (2013). *Thermal performance analysis of a solar water heating system with heat pipe evacuated tube collector using data from a field trial*. Retrieved from Solar Energy, 90 ,17-28: https://www.sciencedirect.com/science/article/pii/S0038092X13000054

Bosch. (2015). *SM CDi Series Technical Specifications*. Retrieved from https://www.bosch-thermotechnology.us/us/media/country_pool/documents/geothermal-heat-pumps-manuals/8733904587-greensource-sm-tech-spec-1-9-15-web_us_1.pdf

Bosch. (2021). *CDi Series HEat Pump and Air Handler Brochure*. Retrieved from https://issuu.com/boschthermotechnology/docs/bosch_sm_split_76h991812b?fr=sZDQwODYwNTkyMA

builditsolar.com. (2022). Retrieved from https://www.builditsolar.com/Projects/Cooling/EarthTemperatures.htm

Cho, R. (2019). *Columbia Climate School* . Retrieved from State of The Planet: https://news.climate.columbia.edu/2019/01/15/heat-pumps-home-heating/

Climate-Data.org. (2022). *Climate-Data.org*. Retrieved from https://en.climate-data.org/north-america/united-states-of-america/north-carolina/asheville-1666/

Dobos, A. P. (2014). *PVWatts Version 5 Manual*. Retrieved from https://pvwatts.nrel.gov/downloads/pvwattsv5.pdf

Dott, R., Haller, M. Y., Ruschenburg, J., Ochs, F., & Bony, J. (2013). *The Reference Framework for System Simulations of the IEA SHC Task 44* . Retrieved from http://task44.iea-shc.org/data/sites/1/publications/T44A38_Rep_C1_B_ReferenceBuildingDescription_Final_Revised_130906.pdf

EUROSTAT . (2020). *Just over 20% of energy used for heating and cooling is renewable* . Retrieved from https://ec.europa.eu/eurostat/web/products-eurostat-news/-/ddn-20201229-

1#:~:text=The%20EU%20share%20of%20energy,2004%20to%2022.1%25%20in%202019.
EUROSTAT. (2019). Retrieved from https://ec.europa.eu/eurostat/statistics-explained/index.php?title=Energy_consumption_in_households
Haller, M. &. (2014). *SOL-HEAP. Solar and Heat Pump Combisystems*. Retrieved from https://www.researchgate.net/publication/272093420_SOL-HEAP_Solar_and_Heat_Pump_Combisystems
HighSeer. (2022). Retrieved from https://www.highseer.com/pages/hvac-load-calculator
Holladay, M. (2017). *Fine Homebuilding*. Retrieved from https://www.finehomebuilding.com/project-guides/insulation/closed-cell-foam-studs-waste
IEA. (2019). *Report extract Heat*. Retrieved from https://www.iea.org/reports/renewables-2019/heat
John Mansfield. (2021b). *Corbond IV Datasheet*. Retrieved from https://www.jm.com/content/dam/jm/global/en/building-insulation/Files/BI%20Data%20Sheets/Resi%20and%20Commercial/JM_BI_Corbond_IV_DS.pdf
Johns Manville. (2021a). *Understanding the GWP, ODP, and 3rd Generation Spray Foam Phase Out*. Retrieved from https://www.jm.com/en/blog/2021/february/understanding-the-gwp--odp--and-gen-iii-spray-foam-phase-out/
Lawrence, M. (2005). *The relationship between relative humidity and the dewpoint temperature in moist air: A simple conversion and applications.* Retrieved from Bull. Amer. Meteor. Soc., 86, 225-233.: http;//dx.doi.org/10.1175/BAMS-86-2-225
Lund, J. (1989). *Ground-source (geothermal) heat pumps*. Retrieved from https://www.researchgate.net/publication/266075259_Ground-source_geothermal_heat_pumps
NOAA. (2022). *National Oceanic and Atmospheric Administration*. Retrieved from https://www.weather.gov/ama/heatindex
NOAA. (2022). *Solar Position Calculator*. Retrieved from https://gml.noaa.gov/grad/solcalc/azel.html
NREL. (2011). *Strategy Guideline: Accurate Heating and Cooling Load Calculations*. Retrieved from https://www.nrel.gov/docs/fy11osti/51603.pdf
Renné, D. (2018). *ICAO Capacity Building Seminar on Low Emissions Aviation Measures 25-26 April 2018*. Retrieved from ICAO: https://www.icao.int/environmental-protection/Documents/2_2_Photovoltaic%20Technologies%20Status%20and%20Trends.pdf
Solcast. (2022). Retrieved from solcast.com
US EIA. (2015). Retrieved from https://www.eia.gov/energyexplained/use-of-energy/homes.php
US EIA. (2021). *How much electricity does an American home use?* Retrieved from https://www.eia.gov/tools/faqs/faq.php?id=97&t=3

US NREL. (2022). *PVWatts Solar Calculator*. Retrieved from https://pvwatts.nrel.gov/pvwatts.php

Vúrge-Vorsatz, D., Cabeza, L. F., Serrano, S., Barreneche, C., & Petrichenko, K. (2015). *Heating and cooling energy trends and drivers in buildings,*. Retrieved from Renewable and Sustainable Energy Reviews, 41, 85-98: https://www.sciencedirect.com/science/article/pii/S1364032114007151#f0015

Widyolar, B., Jiang, L., Bhusal, Y., Brinkley, J., & Winston, R. (2021). *Solar thermal process heating with the external compound parabolic concentrator (XCPC) – 45 m2 experimental array performance, annual generation (kWh/m2-year), and economics*. Retrieved from Solar Energy, 230, 131-150: https://www.sciencedirect.com/science/article/pii/S0038092X21008872

APPENDICES

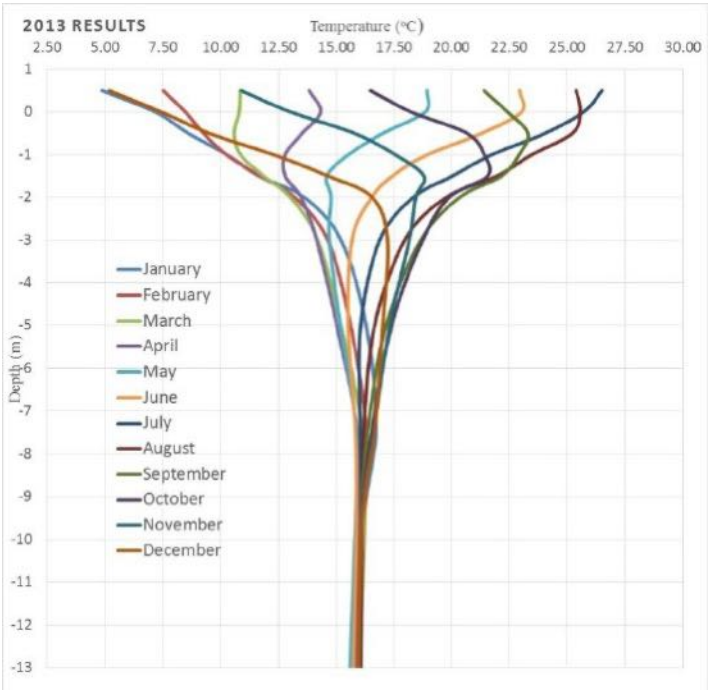

Temperature-Depth Profile over the year in Maslak, Turkey. Notice January exhibits a monotonic and nearly flat increase of temperature with depth, while July exhibits the same behavior in reverse. This behavior is similar to profiles exhibited in other studies and is used as justification for a linear approximation for those months only. (Aydin, Sisman, Gültekin, & Dehghan B., 2015)

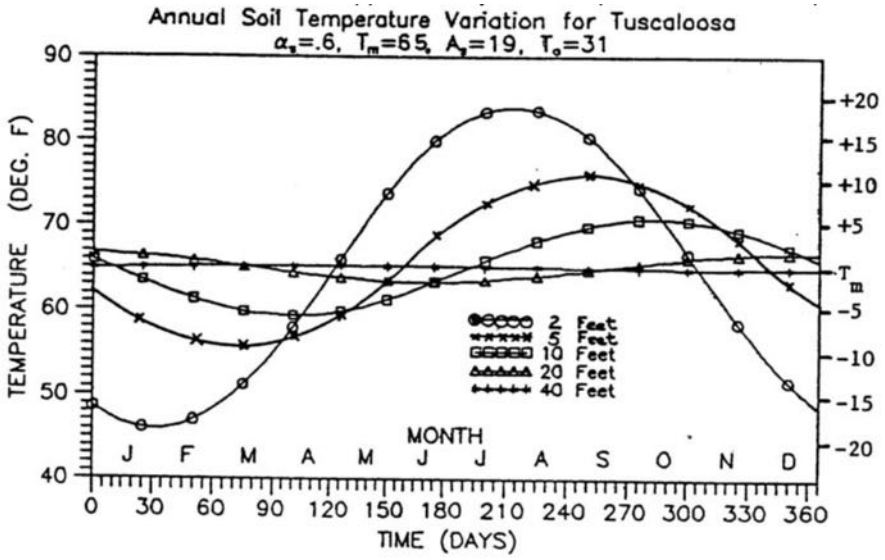

Seasonal Temperature variations at various depths in Tuscaloosa, Alabama, USA. (Lund, 1989)

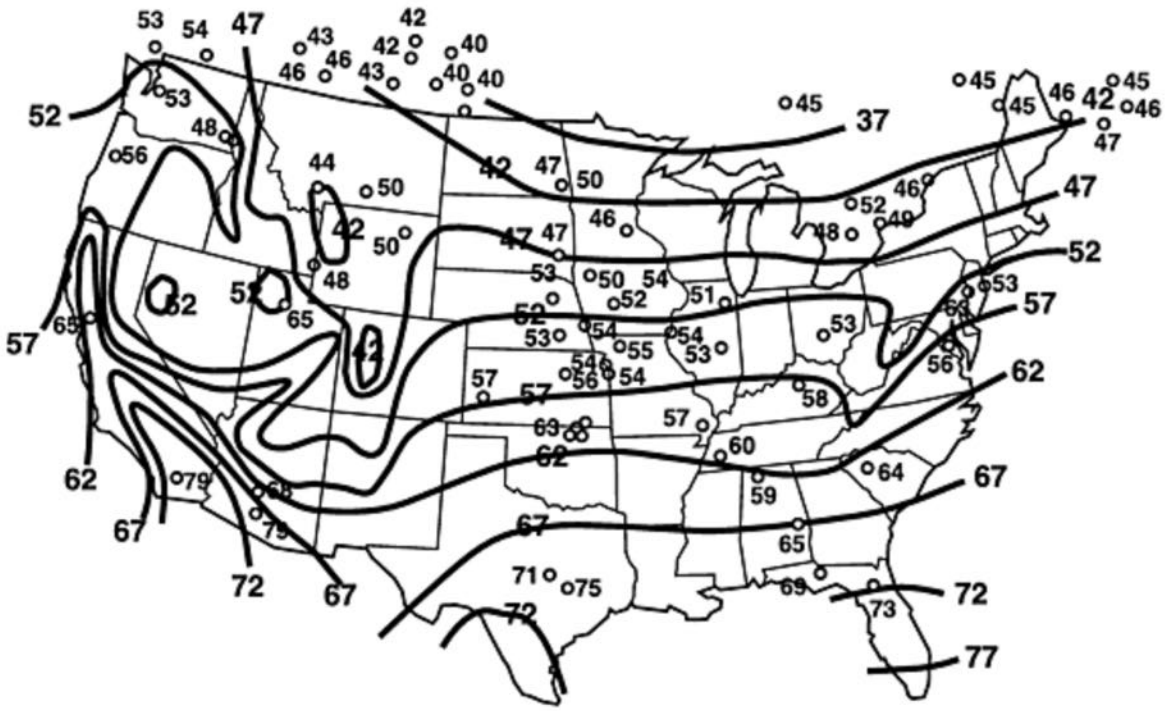

Mean annual earth temperature observations at individual stations, superimposed on well-water temperature contours. Western North Carolina is sandwiched between 62 F (16.6 C) and 57 F (13.8 C) (builditsolar.com, 2022)